THE AMERICAN SOCIETY OF MECHANICAL ENGINEERS
345 E. 47th St., New York, N.Y. 10017

96-GT-140

COMPARISON BETWEEN COMPLETE HILBERT TRANSFORM AND SIMPLIFIED SOLUTIONS OF THE MOORE ROTATING STALL MODEL

Gianmario L. Arnulfi
University of Udine
Dipartimento di Energetica e Macchine
Udine, Italy

Fabio L. Ghiglino, Aristide F. Massardo
University of Genova
Istituto di Macchine e Sistemi Energetici
Genova, Italy

ABSTRACT

The main objective of this work is the analysis and the comparison between different methods utilised to solve the Moore rotating stall model. To date only simplified relations between the axial flow perturbation g and the transverse one h have been utilised and presented in literature, such as $h' = -g$ or the truncated Fourier series. On the contrary, in this paper the accurate relation given by the Hilbert Transform is utilised, and to improve the numerical stability of the method a new expression of the first derivative of transverse flow coefficient perturbation is proposed and utilised.

A complete and detailed comparison between the results of the simplified methods and the solution proposed here is presented. This comparison is extended to a wide range of geometrical and physical compressor parameters, and it allows the accuracy of simplified approaches to be tested.

Finally, a correlative approach estimating overall rotating stall effects based on the complete solution proposed here is presented. It allows rotating stall influence to be quickly and easily taken into account in several axial compressor areas (design, optimisation, active control, etc.).

NOMENCLATURE

A	amplitude of harmonics
AR	compressor characteristic aspect ratio
E	energy coefficient
e	exit duct lag parameter
F	stall propagation speed and wheel speed ratio
f	frequency
g	axial flow coefficient perturbation ($\varphi - \Phi$)
h	transverse flow coefficient perturbation
N	number of results
P	flow perturbation potential
R	regression coefficient
s	compressor stages lag parameter
v	guide vanes lag parameter
x	axial coordinate
δ	difference real/axisymmetric compressor curve
ϑ	circumferential coordinate
λ	overall lag parameter
Φ	average flow coefficient
φ	flow coefficient
Ψ	pressure coefficient
ψ	axisymmetric pressure coefficient

Superscripts and subscripts

a	accurate solution
c	correlative model
n	number of harmonics
p	compressor characteristic peak point
s	simplified solution
v	compressor characteristic valley point
0	referred to standard condition
$'$	ϑ derivative
$*$	normalised with respect to peak-to-valley value
$**$	normalised with respect to mean g^2 value

INTRODUCTION

The importance of the simulation of rotating stall and the evaluation of the influence of that phenomenon on the multistage axial compressors performance are well known and have been stud-

Presented at the International Gas Turbine and Aeroengine Congress & Exhibition
Birmingham, UK — June 10-13, 1996
This paper has been accepted for publication in the Transactions of the ASME
Discussion of it will be accepted at ASME Headquarters until September 30, 1996

ied by several authors (e.g. Greitzer 1976, Moore 1984, Day 1991, Cumpsty and Greitzer 1982). In literature various models are proposed to modelise rotating stall phenomenon, but the Moore model seems to provide the most complete approach; it allows the shape of the stall cell, the propagation speed and the actual performance curve to be determined, and it only deals with compressor data that can be easily obtained.

In literature only simplified solutions of this model have been presented: the most commonly used relation correlating the axial g and transverse h flow perturbations is $h' = -g$ proposed by Moore (1984), while some authors utilise a truncated form of the corresponding Fourier series (Mc Caughan, 1989).

In this work, the solution of the rotating stall model proposed by Moore is carried out utilising the complete set of equations without additional simplifying hypotheses for the relationship between h and g. In this way the complete Hilbert transform of the perturbations is taken into account in the method here presented. To improve the stability and the reliability of the proposed solution a new expression for the first derivative of transverse flow perturbation (h') has been proposed and extensively utilised.

Based on the method described here, a complete in-depth comparison between the accurate and the simplified results is made for a wide range of compressor configurations. In this way, the accuracy of the different simplified relations is clearly stated.

Since the resolution of the Moore model including Hilbert transform is time consuming, the results of the accurate calculation have been utilised to develop a new correlative approach for the evaluation of the overall effects of rotating stall: propagation speed F and alterations δ of the compressor axisymmetric performance curve. The correlation, which is, in most cases, as accurate as traditional simplified models, might be useful when quick a response is needed, such as in the compressor control field or compressor design optimisation problem.

MATHEMATICAL AND NUMERICAL MODEL

In this study, we adopt the mathematical approach to modelise rotating stall proposed by Moore (1984); Moore introduced four main hypotheses to get the final form of his model:

1) incompressible flow through the compressor;
2) irrotational flow in the inlet duct;
3) negligible radial effects in the flow;
4) negligible losses at the IGV entrance, due to the flow angular disturbance present at the inlet.

Moreover rotating stall is studied in a moving frame, rotating with the stall cell; in this way the rotating stall in the turbomachine is steady.

The final equations representing rotating stall are:

$$\delta = \left[\psi(\varphi) - \psi(\Phi)\right] - \lambda \cdot g'(\vartheta) + e \cdot F \cdot h(\vartheta) \qquad (1)$$

where $\delta = \Psi(\Phi) - \psi(\Phi)$ and $\lambda = s/2 - F(s+v)$

$$h(\vartheta) = -\frac{1}{\pi}\int_{-\infty}^{+\infty} \frac{g(\xi)}{\vartheta - \xi}\, d\xi \qquad (2)$$

Equation (1) represents the sum of pressure rise contribution of every component of the compressor (i.e. inlet duct, inlet guide vanes, stages etc.), and Eq. (2) gives the relation existing between the axial flow perturbation g and the transverse one h (Takata and Nagano, 1972). In addition, it is imposed that the mean value of g and h must be zero. In this way δ is the unknown to calculate, e, s and v are fixed parameters, and F, g and h are variables to iterate.

In the Eq. (1) the axisymmetric characteristic curve ψ is present; this curve represents the compressor characteristic in the absence of rotating stall for every mass-flow condition. As suggested by Moore (1984) the axisymmetric characteristic can be obtained in an experimental way by utilising high-loss screens at the inlet and outlet of the turbomachine to eliminate flow distortion. In this study, the S-shaped cubic curve proposed by Koff and Greitzer (1985) is utilised.

Equation (1) is usually derived with respect to the circumferential coordinate ϑ

$$0 = \left.\frac{d\psi}{d\varphi}\right|_{\Phi+g} \cdot g'(\vartheta) - \lambda \cdot g''(\vartheta) + e \cdot F \cdot h'(\vartheta) \qquad (3)$$

Since g and h for physical reasons are periodic functions, Eq. (2) can be written as

$$h(\vartheta) = -\frac{1}{\pi}\int_{0}^{2\pi} \frac{dg(\xi)}{d\xi} \ln\left|\sin\frac{\xi - \vartheta}{2}\right| d\xi \qquad (4)$$

The use of Eq. (4) can be cumbersome, so many proposals for simplified forms of g-h relation were made. Starting from the potential of the flow perturbation developed as a Fourier series (note that the potential exists since the flow is irrotational and incompressible upstream)

$$P(x, \vartheta) = \sum_{n=1}^{+\infty} \frac{1}{n} e^{nx}\left(a_n \sin n\vartheta + b_n \cos n\vartheta\right) \qquad (5a)$$

g and h are obtained as

$$g(\vartheta) = \left.\frac{\partial P}{\partial x}\right|_{x=0} = \sum_{n=1}^{+\infty} \left(a_n \sin n\vartheta + b_n \cos n\vartheta\right) \qquad (5b)$$

$$h(\vartheta) = \left.\frac{\partial P}{\partial \vartheta}\right|_{x=0} = \sum_{n=1}^{+\infty} \left(a_n \cos n\vartheta - b_n \sin n\vartheta\right) \qquad (5c)$$

Many authors use Eq. (5b) and (5c) truncated at the n^{th} term to calculate the rotating stall phenomenon.

Moore himself proposed a simplified relation for his model:

$$h'(\vartheta) = -\, g(\vartheta) \qquad (6)$$

Equation (6) is equivalent to Eq. (4) only if g is a purely harmonic function. Equation (6) is true for the first terms of Fourier series (Eq. 5), but it can also relate functions that are not necessarily truncated Fourier series (Moore, 1984, page 328 Fig. 2). In this paper for the simplified solution g is not obtained by Eq. (5) with n=1.

Here the complete Hilbert transform relation is used to avoid the approximation given by Eq. (5a), (5b) and (6), but in Eq. (3) the first

derivative of h is needed:

$$h'(\vartheta)=\frac{dh(\vartheta)}{d\vartheta}=-\frac{1}{\pi}\frac{d}{d\vartheta}\left(\int_0^{2\pi}\frac{dg(\xi)}{d\xi}\ln\left|\sin\frac{\xi-\vartheta}{2}\right|d\xi\right) \qquad (7)$$

In this form h' is numerically difficult to treat; in fact in some zones the integral function presents very steep slopes, and so the derivative shows singular values. To avoid the influence of the singular point a new expression for h' is obtained by substitution in Eq. (7) of:

$$\eta=\frac{\vartheta-\xi}{2} \qquad G(\vartheta-2\eta)=\frac{dg(\xi)}{d\xi} \qquad (8)$$

and dividing into two parts the integral to avoid the singular value of the integrand function for $\xi=\vartheta$

$$h'(\vartheta)=-\frac{1}{\pi}\left[-2\frac{d}{d\vartheta}\int_{\vartheta/2}^{\vartheta/2-\pi}G(\vartheta-2\eta)\ln|\sin\eta|\,d\eta\right] \qquad (9a)$$

$$h'(\vartheta)\cong-\frac{1}{\pi}\left\{2\frac{d}{d\vartheta}\left[\int_{\vartheta/2-\pi}^{-\varepsilon}G(\vartheta-2\eta)\ln|\sin\eta|\,d\eta+\int_{\varepsilon}^{\vartheta/2}G(\vartheta-2\eta)\ln|\sin\eta|\,d\eta\right]\right\} \qquad (9b)$$

and since the integrand functions in Eq. (9b) are bounded and continuous, and ε is so small that the neglected areas are nearly zero, letting

$$J(\eta,\vartheta)=G(\vartheta-2\eta)\ln|\sin\eta| \qquad (10)$$

Eq. (9b) becomes

$$h'(\vartheta)=-\frac{1}{\pi}\left\{2\left[\int_{\vartheta/2-\pi}^{-\varepsilon}\frac{\partial J}{\partial\vartheta}d\eta-\frac{1}{2}J\left(\frac{\vartheta}{2}-\pi,\vartheta\right)+\int_{\varepsilon}^{\vartheta/2}\frac{\partial J}{\partial\vartheta}d\eta+\frac{1}{2}J\left(\frac{\vartheta}{2},\vartheta\right)\right]\right\} \qquad (11)$$

Since the function J is periodic of period 2π, if only one stall cell exists, substituting again Eq. (8) and Eq. (10) into Eq. (11) one obtains:

$$h'(\vartheta)=-\frac{1}{\pi}\left(\int_0^{2\pi}\frac{d^2g(\xi)}{d\xi^2}\ln\left|\sin\frac{\xi-\vartheta}{2}\right|d\xi\right) \qquad (12)$$

The second derivative of the axial perturbation g is calculated from the previous iteration; the first one utilises the Moore simplified relation (Eq. 6), as suggested by Saju (1985). Utilising Eq. (12) h' presents a continuous behaviour without singular values, increasing the convergence speed of the solution.

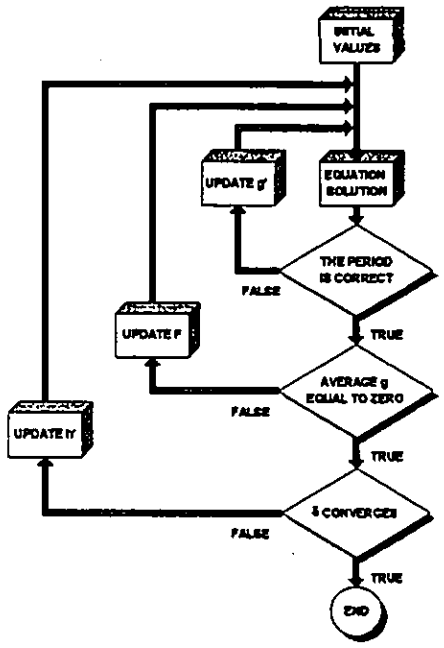

Fig. 1 - Flow chart of the accurate model

Numerically the problem is the solution of a non linear second order ordinary differential equation (a boundary value one), solved by a shooting method, using an explicit fourth order Runge-Kutta solver with Simpson constants and variable step.

The flow-chart of the accurate solution code is shown in Fig. 1. The inner loop controls the period value changing g' at $\vartheta=0$ by the bisection method (periodicity is intrinsic with the definition of g). The second loop verifies if the integral of g is nearly zero; if not, the value of the stall cell speed propagation F is changed by the secant method. The external loop controls the value of δ (difference between the real and the axisymmetric compressor characteristic): h' is updated by the recursive method until the differences of δ values of the last two calculations are inside a prescribed tolerance.

The accurate solution is obtained by starting from the simplified one; this implies that some numerical problems can arise in the internal loop if the exact value of the period is not quickly reached, because of matching difficulties with the simplified solution which is, for one stall cell, a periodic function of period 2π. These numerical problems grow for high characteristic aspect ratio AR (see Eq. 17).

The code, written in Fortran language, runs on a Pentium 90 PC, and it takes about 20 seconds to get the simplified solution and 100 times more for the complete one.

DISCUSSION OF RESULTS

Utilising the model described and the code developed, the behaviour of axial multistage compressors, operating under rotating stall conditions, is evaluated. The lag parameters are evaluated with the method given by Hynes et al. (1985), while the axisymmetric curve and the mass flow rate are normalised to make possible an easy comparison among different compressors in the following way:

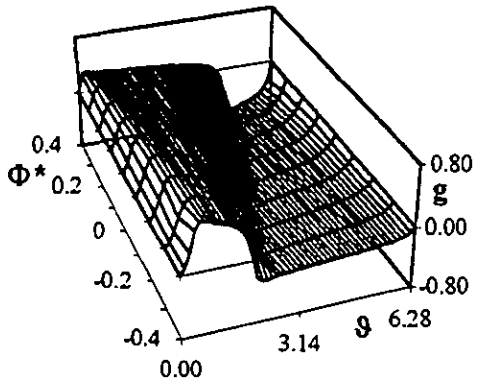

Fig. 2a - Influence of Φ* and ϑ on *g* behaviour obtained with accurate solution.

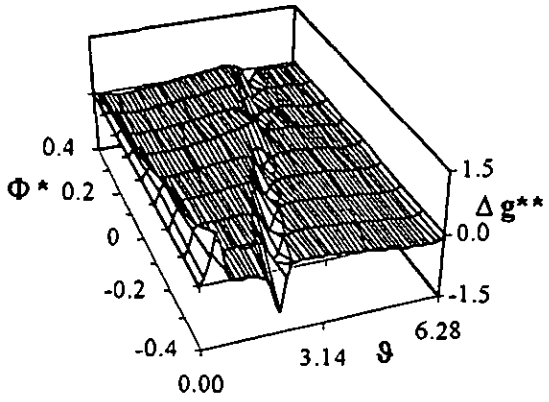

Fig. 2b - Influence of Φ* and ϑ on the normalised difference of *g* function (accurate and simplified solution).

$$\Phi^* = \frac{\Phi - 0.5\cdot(\Phi_p + \Phi_v)}{\Phi_p - \Phi_v}; \quad \Psi^* = \frac{\Psi - 0.5\cdot(\psi_p + \psi_v)}{\psi_p - \psi_v} \quad (13)$$

All the flow and characteristic coefficients are both calculated with the simplified Moore relation (Eq. 6) and with the accurate one (Eq. 4) given by the Hilbert transform. This allows a quick comparison in every flow condition to be obtained.

The first comparison between the two methods is carried out for the axial flow perturbation in Fig. 2, where the configuration of the considered turbomachine is shown in table 1 (standard configuration). The trend of g versus Φ^* and ϑ is shown in Fig. 2a, while the difference between the accurate and simplified solutions is shown in Fig. 2b.

Φp-Φv	AR	v	s	e
0.45	0.7	0.15	1.4	1.75

Table 1 - Standard Compressor Parameters.

In this way, it is easy to understand how accurate the simplified method is. The gap between the two solutions for g is normalised with respect to a sort of "mean" axial perturbation coefficient

$$\sqrt{2E} = \sqrt{\overline{g^2}} \quad (14)$$

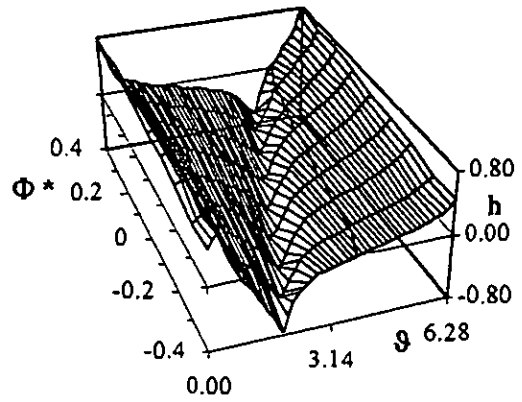

Fig. 3a - Influence of Φ* and ϑ on *h* behaviour obtained with accurate solution.

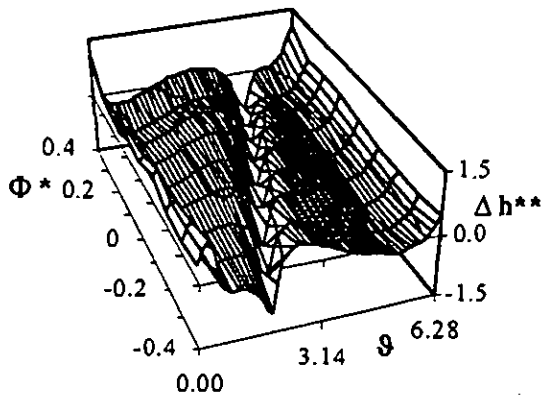

Fig. 3b - Influence of Φ* and ϑ on the normalised difference of *h* function (accurate and simplified solution).

where E is the energy related to the stall cell and is defined as:

$$E = \frac{1}{4\pi}\int_0^{2\pi} g^2(\vartheta)d\vartheta \quad (15)$$

and

$$\Delta g^{**}(\vartheta) = \frac{g_a(\vartheta) - g_s(\vartheta)}{\sqrt{2E}} \quad (16a)$$

As shown in Fig. 2, Δg^{**} is not large, except near the peaks (maximum and minimum) of the g function where the variation is approximately 100%. This is not negligible especially for the zone where g is minimum, in fact there is the possibility of falling in a back-flow zone, while the underestimated values given by the Moore simplification do not represent this flow behaviour, as already discussed by Arnulfi et al. (1995).

The same analysis is done for the transverse flow perturbation shown in Fig. 3a and the difference between the two solutions shown in Fig. 3b. Again the error is normalised as before and now one obtains:

$$\Delta h^{**}(\vartheta) = \frac{h_a(\vartheta) - h_s(\vartheta)}{\sqrt{2E}} \quad (16b)$$

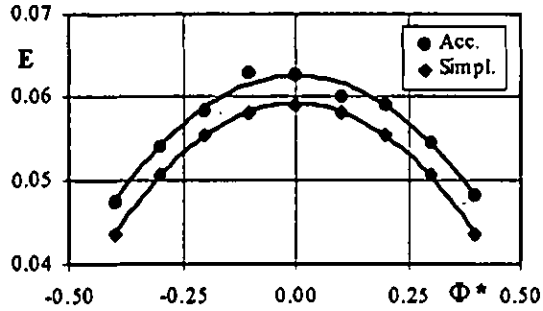

Fig. 4 - Comparison between simplified and accurate stall cell energy.

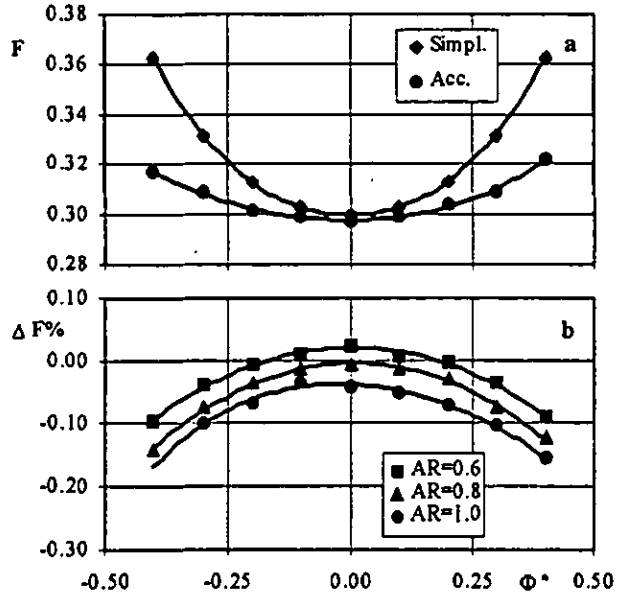

Fig. 5 - Comparison between simplified and accurate stall cell speed: a) standard condition; b) AR influence.

In this case the gap between the two solutions is large for every operating condition and, since h gives information about the stall cell propagation around the annulus and the way in which flow goes in and out from the stall condition, this is not a negligible detail.

To complete this first part of the comparison, the behaviour of the energy related to the stall cell changing with the mass flow rate Φ^* is shown in Fig. 4. Both the simplified and the accurate solution present the same trend: in fact, as expected, this energy decreases as the compressor approaches stable operating or back flow conditions, where the stall cell vanishes. On the contrary, the simplified solution underestimates the accurate values with an error of about 7%; that is why the stall cell shape calculated by the Moore relation $h' = -g$ is smoother than the shape calculated by the Hilbert transform, as shown in Fig. 2.

The comparison is then carried out on the overall characteristic of rotating stall. The non-dimensional propagation speed of the stall cell versus Φ^* for the two methods is shown in Fig. 5a; one can see that the stall cell moves, around the annulus, more quickly as it approaches nearer and nearer to the negative slope legs of the characteristic ($\Phi^* \equiv \pm 0.5$). Moreover, the curve obtained by the Moore relation overestimates the one obtained by the Hilbert transform.

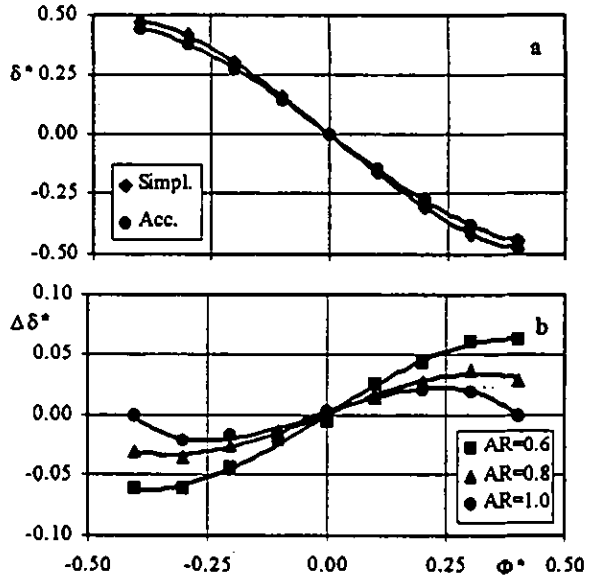

Fig. 6 - Comparison between simplified and accurate δ* values: a) standard condition; b) AR influence.

The difference between the accurate and the simplified solution, normalised with respect to the accurate one, is shown in Fig. 5b for several aspect ratio values AR, defined as:

$$AR = \frac{\Psi_p - \Psi_v}{\Phi_p - \Phi_v} \qquad (17)$$

The parameter AR is representative of the compressor curve steepness, so when AR grows, the compressor characteristic becomes steeper. One can see that the gap for F between the two solutions increases as AR increases and as one approaches the recovery or back flow zone; this gap can reach 15% and more.

The behaviour of the coefficient δ^*, the difference between the stalled and the axisymmetric characteristic, is reported in Fig. 6a. δ^* is a decreasing function with Φ^*, becoming negative for positive values of Φ^*; this means that the stalled curve is always less steep than the axisymmetric one.

The difference between the two analysed methods is shown in Fig. 6b for different AR values. It is clear that the simplified solution overestimates the accurate one for every mass flow rate; this difference increases as the compressor goes toward stable or back flow condition, while it decreases for high values of the AR parameter.

Since the coefficient δ^* is referred to the overall outlet conditions of the compressor, it is important to know the influence of the single parts of the machine and the influence of the two methods of solution during the calculation. So the contributions of the single compressor components for pressure rise, for three different values of Φ^*, are shown in Fig. 7. One can observe that through the inlet duct there is a pressure drop due to flow acceleration and pressure losses, except for the circumferential stalled portion where the pressure of course does not decrease. The IGV also shows a slight pressure drop, but within two narrow zones there is a pressure rise due to the crossing of the entrance plane of the IGV and due to inertial effects, function of h^2. The compressor stages of course provide a pressure increase except for the stalled blades that cannot operate well. Finally, in the outlet duct the circumferential pressure trend is governed by the boundary conditions: stages outlet and downstream ple-

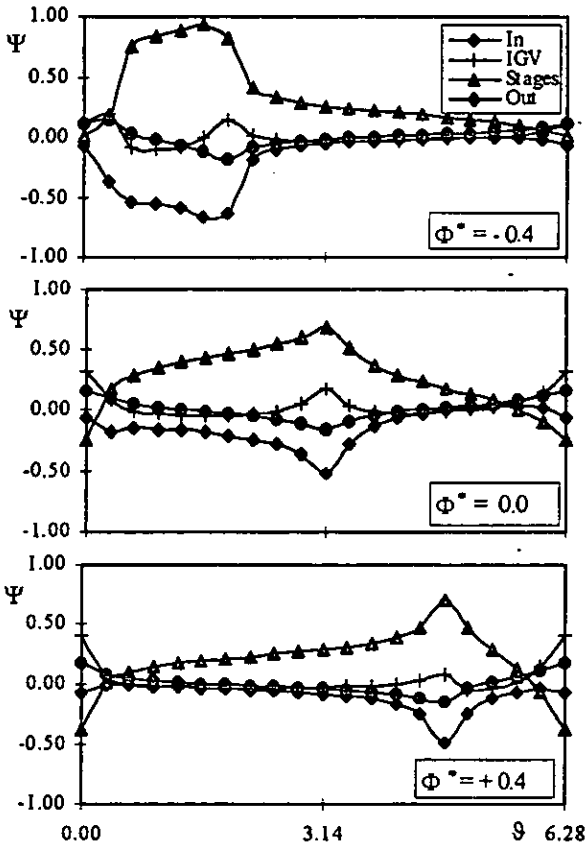

Fig. 7a - Pressure rise of the single components obtained by the accurate method (standard condition).

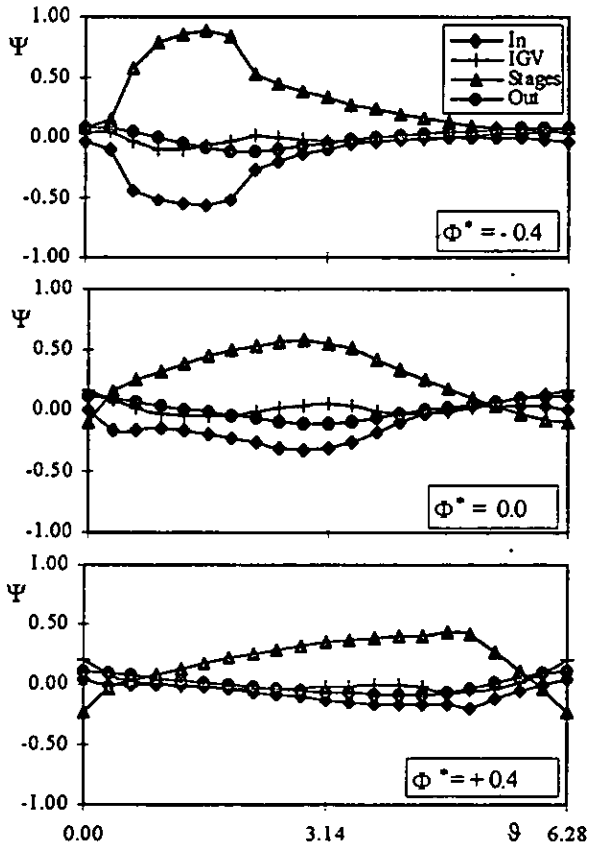

Fig. 7b - Pressure rise of the single components obtained by the simplified method (standard condition).

num conditions. The pressure rise of the single compressor components calculated by the Hilbert transform is shown in Fig. 7a, while the ones calculated by the simplified relation are shown in Fig. 7b.

The results obtained by the two methods have the same qualitative trend, but there are strong differences for the maximum and minimum values, and the corresponding gradient of the pressure functions; this kind of behaviour was already shown by g and h in Fig. 2 and 3. For this reason, using the simplified approach, information on sudden pressure drops or pressure increases along ϑ could be lost, as can be observed for all the components here analysed and especially for the inlet duct and the compressor stages.

A parametric analysis of the overall characterisiic of the rotating stall phenomenon is carried out and shown in Fig. 8 to complete the study on the accurate solution. One can see in Fig. 8b and 8c that propagation speed is quite sensitive to stage and exit duct geometry. In fact F increases as s increases and e decreases, and slightly decreases when the IGV lag parameter ν grows (Fig. 8a). The characteristic curve of the compressor (represented by gap δ^*) and the cell shape (represented by the energy E) are not influenced by the lag parameters, but a slight change, if the exit geometry varies (e), is noted (Fig. 8c).

FFT analysis

Many authors utilise a truncated form of the Fourier series of g and h (see Eq. 5b and Eq. 5c) to calculate the rotating stall effects. For this reason an FFT analysis of the accurate results is made, then a comparison between g and h calculated by the Hilbert transform and g and h calculated using the first 10, 15 and 20 harmonics obtained by the FFT analysis, is carried out. This comparison is shown in Fig. 9 for two different mass flow rate conditions, the gap is normalised in the same way as Fig. 2b and 3b, but this time

$$\Delta g^{**}(\vartheta) = \frac{g_a(\vartheta) - g_n(\vartheta)}{\sqrt{2E}}, \quad \Delta h^{**}(\vartheta) = \frac{h_a(\vartheta) - h_n(\vartheta)}{\sqrt{2E}} \qquad (18)$$

where n is the number of harmonics.

Considering less than 10 harmonics, agreement with the complete solution is too poor still, the gap being of the order of magnitude of the mean g coefficient (over 30%), and it needs more than 20 harmonics to differ less than 5%, even in the simplest case of h, for Φ^*=0.0.

The FFT analysis is then carried out changing the parameter AR and the lag parameters ν, s and e, to obtain a complete comparison with the methods utilising the truncated Fourier series (Fig. 10). An FFT analysis is also carried out for the simplified solution to show the lack of accuracy introduced with respect to the accurate one (Fig. 11). It is important to remember that the simplified solution has been obtained by the Moore relation (Eq. 6), but not as truncated Fourier series. As shown in Fig. 10, for the accurate solution, since h is the Hilbert transform of g, their spectra coincide (equal frequency and amplitude, only phase differs), while (Fig. 11) two different spectra are obtained by the simplified solution. At $\Phi^* = 0.0$ only odd harmonics occur and their amplitude smoothly decreases down to zero, close to 1/30 of a revolution. The closer negative slope characteristic

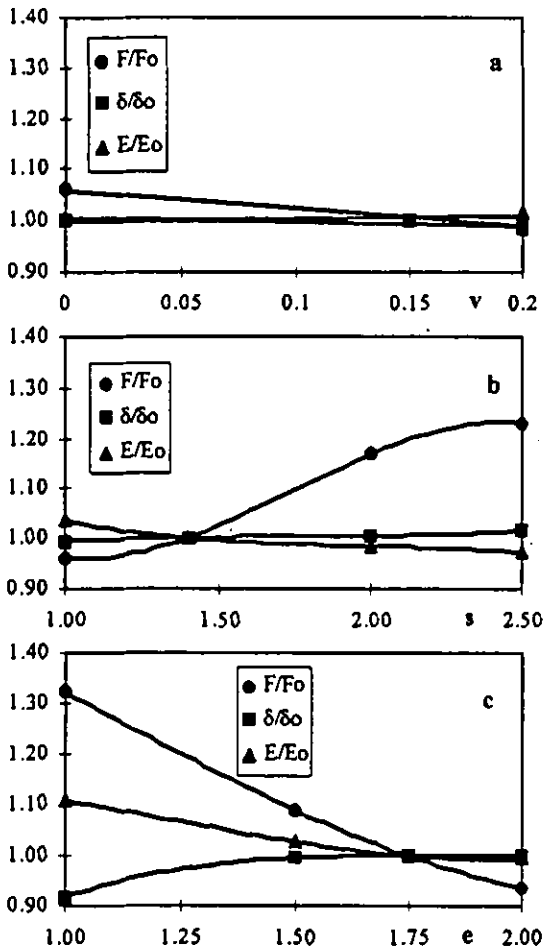

Fig. 8 - Parametric analysis: a) influence of IGV lag parameter; b) influence of stages lag parameter; c) influence of outlet duct parameter.

legs, the more complex the spectra are, with even harmonics too and irregular amplitude trends. This is not surprising because of the stall cell shape behaviour (Arnulfi et al., 1995), but unfortunately, from the stall recovery point of view, the high Φ^* zone is the most interesting. By varying characteristic shape (AR) and lag parameters (v, s and e) no qualitative changes occur in the spectra, but amplitudes are slightly different. Comparison with the simplified solution shows a rather good agreement as to g, being responsible for stall cell shape, but a very poor one as to h, being related to local propagation speed.

A TIME EFFECTIVE MODEL

The resolution of the rotating stall model including the Hilbert transform is CPU-time expensive, while in some applications, such as active compressor control or optimisation problems for compressor design, a quicker and not iterative procedure should be necessary. For this reason, using the accurate method presented in this paper, a new correlative approach for the overall compressor performance (pressure coefficient and propagation speed) is obtained and described by the relations:

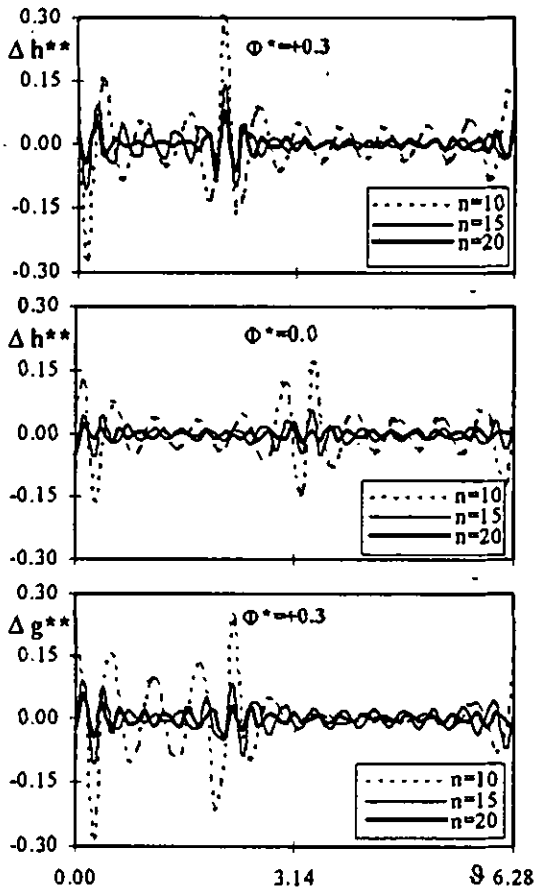

Fig. 9 - Comparison for g and h obtained by accurate and truncated solutions (n = harmonics number).

$$\delta^* = f_1(\Phi^*, AR, e, s, v) \quad (19a)$$

$$F = f_2(\Phi^*, AR, e, s, v) \quad (19b)$$

and in this case the equations are:

$$\delta^* = K_1\Phi^* + K_3\Phi^{*3} \quad (20a)$$

$$F = K_0 + K_2\Phi^{*2} + K_4\Phi^{*4} \quad (20b)$$

where

$$K_j = K_{j0} + K_{j1}v + K_{j2}s + K_{j3}e + K_{j4}AR \quad (20c)$$

for $j = 0 \div 4$

Their numerical values are shown in table 2

K_{00}= 0.340	K_{01}= - 0.105	K_{02}= 0.005	K_{03}= - 0.103	K_{04}= 0.103
K_{10}= - 2.011	K_{11}= - 0.062	K_{12}= - 0.034	K_{13}= - 0.220	K_{14}= 0.263
K_{20}= - 0.213	K_{21}= 1.355	K_{22}= - 0.032	K_{23}= - 0.008	K_{24}= - 0.367
K_{30}= 19.040	K_{31}= 0.838	K_{32}= 0.014	K_{33}= - 9.182	K_{34}= - 1.209
K_{40}= 2.863	K_{41}= - 13.27	K_{42}= - 0.549	K_{43}= 1.555	K_{44}= - 3.932

Table 2 - Coefficients of correlation

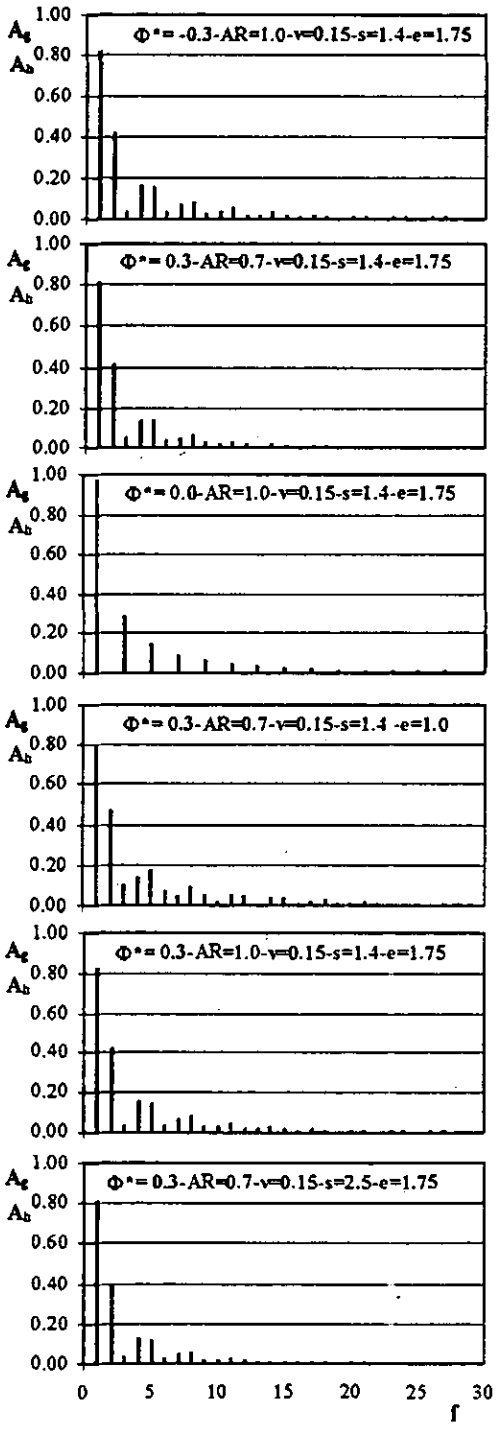

Fig. 10 - FFT analysis of the accurate solution at different flow rate and geometrical parameters.

The constants have been obtained by a least squares method, based on the results of the accurate model code.

This correlative approach should be used in the following range:

$-0.4 < \Phi^* < +0.4$ $\quad +0.5 < AR < +1.0$

$+1.0 < e < +2.0$ $\quad +1.0 < s < +2.5$

$+0.0 < v < +0.2$

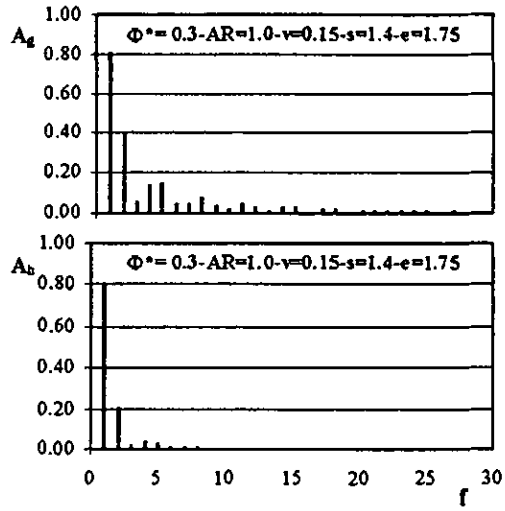

Fig. 11 - FFT analysis of the simplified solution (standard condition).

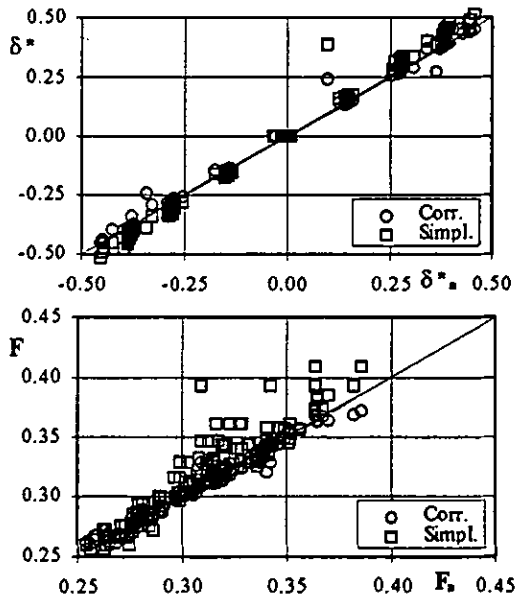

Fig. 12 - Comparison between accurate , simplified (Eq. 6) and correlative (Eq. 17 and 18) approaches.

Since one can easily estimate axisymmetric characteristic and lag parameters (Hynes et al., 1985), immediately these equations give an approximate value of δ^* and F for every compressor operating in any stalled condition. As one can see in Fig. 12, the estimation is good (the regression coefficients, defined in Eq. 21, are $R(\delta^*) = 0.020$ and $R(F) = 0.005$) and, above all, not worse than that obtained by traditional simplified methods.

$$R(y) = \sqrt{\frac{\sum_{i=1}^{N} [y_a - y_c]_i^2}{N-1}} \qquad (21)$$

CONCLUSIONS

Moore, utilising the complete Hilbert transform relation between the axial flow perturbation g and the transverse one h.

A full comparison between the data given by the accurate model and the ones given by the simplified relation was made. The main results of this comparison are:

— the axial perturbations obtained by the two models are quite similar, except near peak values, while the transverse flow perturbation shows a large difference (Fig. 2, 3);
— the energy coefficient E calculated by the simplified model underestimates the energy related to the stall cell given by the accurate one (Fig. 4);
— δ^* and F calculated by the simplified solution always overestimate the ones calculated by the Hilbert transform (Fig. 5, 6);
— the single component pressure rise contribution calculated by the two models shows a similar trend, but the simplified relation does not capture well the sudden pressure drops (Fig. 7);
— from a FFT analysis it turns out that more harmonics are needed to represent the flow perturbation as the mass flow rate approaches recovery or back flow conditions (Fig. 10);
— only a slight change in the amplitudes is produced by varying the aspect ratio values AR and the lag parameters v, s and e (Fig. 10).

Finally a new analytical formulation for δ^* and F has been proposed, utilising the data given by the accurate model. In this way a quick and easy response on overall rotating stall effects is obtained (Fig. 12).

ACKNOWLEDGEMENTS

This research was supported by MURST (Italian Ministry of University and Research - 40% funds and 60% funds)

The authors wish to thank the reviewers for their valuable suggestions.

REFERENCES

Arnulfi, G.L., Ghiglino, F.L., Massardo, A.F., 1995, "A Complete Solution of Non-linear Equations for Rotating Stall in Axial Multistage Compressors", *2nd International Conference on Pumps and Fans*, Beijing, Popular Republic of China, Oct. 17-20.

Cumpsty, N.A., Greitzer, E.M., 1982, "A Simple Model for Compressor Stall Cell Propagation", *ASME Journal of Engineering for Power*, vol. 104, p. 170-176.

Day, I. J., 1991, "Stall Inception in Axial Flow Compressors", ASME Paper 91-GT-86.

Greitzer, E. M., 1976, "Surge and Rotating Stall in Axial Flow Compressors", ASME *Journal of Engineering for Power*, Vol. 98, N° 2, pp. 190-217.

Hynes, T. P., Chue, R., Greitzer, E. M., Tan, C. S., 1985, "Calculations of Inlet Distortion Induced Compressor Flowfield Instability", *AGARD Conference Proceedings No. 400.*

Koff, S. G., Greitzer, E. M., 1984, "Stalled Flow Performance for Axial Compressors: Axisymmetric Characteristic", ASME paper 84-GT-93.

McCaughan, F.E., 1989, "Numerical Results for Axial Flow Compressor Instability", *ASME Journal of Turbomachinery*, vol. 111, pp. 434-441.

Moore, F. K., 1984, "A Theory of Rotating Stall of Multistage Axial Compressors", *ASME Journal of Engineering for Gas Turbines and Power*, Vol. 106, pp. 313-336.

Saju, T.J., 1985, "Effect of Compressor Parameters on Rotating Stall", MSc Thesis, Cornell University.

Takata, H., Nagano, S., 1972, "Non-linear Analysis of Rotating Stall", *ASME Journal of Engineering for Power*, Oct., pp. 279-293.